Hindawi
Advances in Civil Engineering
Volume 2019, Article ID 7319379, 14 pages
https://doi.org/10.1155/2019/7319379

Research Article

Analysis of a Methodology for Torsional Test under Normal Stress and Shear Performance for Asphalt Mixtures

Jun Xie,[1,2] **Yiqun Zhan**,[1] **and Yifan Wang**[1]

[1]*School of Traffic and Transportation Engineering, Changsha University of Science & Technology, Changsha 410114, China*
[2]*National Center for Asphalt Technology at Auburn University, Auburn, AL 36830, USA*

Correspondence should be addressed to Jun Xie; howardxj@csust.edu.cn

Received 24 April 2019; Revised 27 June 2019; Accepted 23 November 2019; Published 10 December 2019

Academic Editor: Alessandro Palmeri

Insufficient shear performance in an asphalt mixture is a primary reason for rutting deformation and pavement surface longitudinal cracking. Thus, it is important to choose a suitable shear test method to evaluate shear performance in an asphalt mixture. Current testing methods mainly evaluate the bonding strength between asphalt layers, and the current shear test method for an asphalt mixture is disadvantaged by high equipment cost and complicated procedures. Our study proposes a torsional test method under normal stress condition, and evaluation was done for four types of asphalt mixture under different temperature conditions. Through the mechanical analysis, the calculation formulas for shear strength and shear parameters (cohesion and internal friction angle) for the torsional test under a normal stress condition were obtained. Testing results were also obtained for shear strength, shear modulus, and cohesion and internal friction angle of the asphalt mixtures. Experimental testing indicated that the method was able to provide repeatable results for the shear resistance of asphalt mixtures at different temperatures and also reflected the difference in shear performance of the various asphalt mixtures and the influence of temperature on shear performance. The failure mode of the specimen was the appearance of an oblique crack of about 45° from the vertical axis after the specimen was destroyed, which accorded with shear failure characteristics. A shear fatigue model was obtained considering different shear stress levels. The torsional test method under normal stress formed a compression-shear action on the specimen by applying torque and normal stress and was used to evaluate the shear performance of the asphalt mixtures.

1. Introduction

With the rapid growth of traffic volume and the continuous development of heavy-duty transportation in China, various damages have occurred to asphalt pavement on expressway and trunk highway. Among them, permanent deformation (rutting) and pavement surface longitudinal cracking are the two main forms of asphalt pavement damage currently seen in China.

Permanent deformation (rutting) is a surface depression in wheel paths caused by repeated loading due to heavy traffic loading that causes a progressive accumulation of permanent deformation under repetitive tire pressure. Pavement uplift (shoving) may also occur alongside the rutting. In the initial stage after opening up to traffic, there was the appearance of a one-dimensional rut depth caused by material densification in a depression near the center of the wheel path without an accompanying hump on either side of the depression. This densification of materials was generally caused by excessive air voids or inadequate compaction of pavement layers. More severe premature distortion and rutting failures were related to lateral movements or a plastic flow of materials from wheel loads upon asphalt layers with inadequate shear strength and/or due to large shear stress states from traffic loads. Results of trenching studies from the American Association of State Highway Officials (AASHO) Road Test as well as other test tracks indicated that shear deformation rather than densification was the primary permanent deformation mechanism [1–3].

Pavement surface longitudinal cracking appeared as cracks began to form at the surface of the asphalt concrete

layer and propagated downward with time, which significantly reduces the quality service life of pavement [4]. The causes of pavement surface longitudinal cracking were very complicated. Several possible causes were identified, including tire-pavement contact properties, thermal gradient, thickness of pavement, mixture type, type of binder and gradation of aggregate, aging of mixtures, and construction factors [5–8]. From the perspective of mechanical analysis, various researchers concluded that pavement surface longitudinal cracking was caused by tensile stress rather than shear stresses or the load-induced tensile strains at the edge of the tire caused pavement surface crack initiation [9–11].

The majority of pavement surface longitudinal cracking instances were found in the vicinity of wheel paths, and thus, investigation pursued load-induced tensile stresses and strains in the vicinity of the tire-pavement contact areas. It was also found that surface radial tensile stress induced by wheel loads could cause pavement surface longitudinal cracking and the locations of the maximum surface tensile stress predicted by the mechanistic analysis corresponded very well to the locations of the pavement surface longitudinal cracking observed in the field [12].

Other researchers, however, hold different opinions about the initiation of pavement surface longitudinal cracking. Groenendijk [13] argued that crack propagation in a pavement surface occurs mainly in the shear mode, yielding due to shear stresses that result in shearing cracks. A finite element model analysis showed that load-induced shear strains at the edge of wheels in the vertical plane were higher than the load-induced lateral tensile strains at the same location on the pavement surface. Therefore, the shear strains on the vertical plane played an important role in crack initiation and propagation [14]. Analysis were conducted with nonuniform contact stresses of tire-pavement under standard and heavy-duty loading in asphalt mixture layers and showed that maximum shear stress occurred at the tire edge and maximum shear stress was far more than maximum tensile stress in the surface of the pavement, and this point of peak shear stress was one of the major factors responsible for pavement surface longitudinal cracking initiation and propagation [15–17].

Based on the above overview about the mechanisms of permanent deformation and pavement surface longitudinal cracking, it is essential to determine and specify appropriate asphalt mixtures to provide adequate shear resistant capacity. Additionally, it is important to develop, select, and utilize appropriate experimental approaches to evaluate the shear resistant capacity of asphalt mixtures.

2. Methods of Shear Test Overview

In early days, shear test equipment was lacking, and thus in order to study the rutting resistant ability of an asphalt mixture, Christensen et al. [18] recommended the use of an indirect tensile test and unconfined compression test to obtain cohesion and internal friction angle, while axial compressive strength was obtained by a uniaxial compression test, and tensile strength was obtained by the indirect tensile test. Subsequently, shear strength and parameters were calculated according to the Mohr–Coulomb theory.

Different shear test methods have since been developed, such as the Leutner method [19], which was an early method for determining the internal bonding strength of asphalt layers. Additional methods include Florida shearing apparatus [20], Canada shear strength test [21], and France double shear test [22]. Various test equipment includes Ancona shear testing research and analysis (ASTRA) equipment [23], which was similar to the direct shear box in the geotechnical test, direct shear test device [24], Louisiana interface shear strength tester (LISST) [25], NCAT bond strength device [26], Nottingham shear box [27], and field shear tester (FST) [28]. Test equipment described in the above literature applied normal stress to simulate the actual effect of traffic loads on the pavement structure. The above methods, however, are mainly used to test the bonding strength between asphalt layers.

In the 1950s, a gyratory testing machine (GTM) was invented by the U.S. Army Corps of Engineers to design asphalt mixture, which could be controlled according to the height of the specimen and the actual number of compacting times, and simulated different tire pressure effects by setting different pressures. Based on this, Guler et al. [29] designed a method to evaluate the shear strength of the mixture. However, the method was designed to have a lower asphalt aggregate ratio than usual, and the equipment cost was high, and thus, it was not widely used in China.

Presently, there are several representative shear test methods for an asphalt mixture.

2.1. Triaxial Test. The triaxial test method originated from the soil mechanics test was used for studying asphalt mixture performance in the 1930s. The basic principle was that the asphalt mixture was assumed to be an isotropic homogeneous body, and the specimen was placed in a three-direction stress state by applying a confining pressure and an axial load.

The triaxial test is a compression test with essentially a confined restriction (confining pressure) [30], where the principal axial stress is the main reason for failure in a specimen. The internal friction angle and cohesion of the asphalt mixture are determined by Mohr–Coulomb strength theory. Some researchers [31] concluded that repeated load triaxial tests appear to provide a better measure of rutting characteristics than the creep test.

However, there are some deficiencies in the triaxial test [32]. Brown [33] pointed out that the triaxial test could only apply a tensile stress in one direction, while in actual pavement, there are also lateral and longitudinal tensile stresses. Thrower [34] also pointed out that the states of stress encountered in the upper layers could not be duplicated in triaxial testing. At present, the triaxial test is not the standard test method to determine the shear strength of an asphalt mixture, and it is only recommended as the test method for determination of asphalt mixture shear strength in Chinese specification (JTG E20-2011).

2.2. SST. Permanent deformation was one of the major research focuses of Strategic Highway Research Program (SHRP) [35], and one of the achievements was the development of a simple shear test (SST) method for determining the permanent deformation performance of an asphalt mixture and for rutting depth prediction. During the test, the top and bottom of the asphalt mixture specimen are bonded with clamp plates by epoxy resin, and the upper and lower clamp plates are fixed with a shearing table, while vertical displacement is controlled by using the vertical sensor such that the height of the specimen remains unchanged to ensure that the specimen is subjected to the shear test under equal volume conditions. Applying vertical and horizontal loads to the specimen under high-temperature conditions results in the occurrence of a plastic shear flow deformation. Tests like the repeated shear test at constant height, shear frequency sweep at constant height, and simple shear test at constant height can be performed with this method [36].

Romero and Anderson [37] considered that the results of constant height repeated shear tests in SST showed high variability. Some studies also indicated that the relationship between laboratory test results and field rutting depth was not satisfactory [38]. In addition, the equipment necessary was expensive, and the test procedures were very complex, with difficult maintenance. Thus, such testing was not widely adopted in China, and only some universities and researching institutes had such equipment.

2.3. Hollow Cylindrical Specimens Method. Since it was difficult to utilize existing laboratory equipment to directly apply a shear load, studies looked at the use of hollow cylindrical specimens to perform a shear test by applying a torque or an axial load to an asphalt mixture. This mainly included the following loading modes.

In the first loading mode, a uniform shear stress is applied to a hollow cylindrical specimen by a torque action to measure the shearing parameter. This was first proposed by the University of California at Berkeley to study the dynamic properties of asphalt mixtures [39], but the wall thickness of the specimen was only 12.5 mm, cutting was difficult, and the results for large particle size aggregates were not sufficiently accurate. Rueda et al. [40] improved upon the method by using a specimen, where the wall thickness was 25.4 mm and outer diameter was 12.7 cm. This method could measure linear elastic properties, dynamic shear modulus, and the relaxation modulus of asphalt mixtures under normal stress and torque.

The second loading mode is also known as the coaxial shear test (CAST) [41]. The principle in this test utilizes a hollow cylindrical specimen placed in a cylindrical steel cylinder of suitable size, where the outer part is bonded with the steel cylinder and the inner part of the specimen is bonded with a steel shaft with epoxy resin. After bonding, pavement surface shear stress was simulated by applying a load to the bonded steel shaft. However, this method was still an indirect test method. At the same time, since the specimen was bonded to the steel shaft and the outer steel cylinder by epoxy resin, the adhesion of the epoxy resin had a certain influence on the experimental results. In addition, when the aggregate particle size was large, the test results would be affected.

The third loading mode was achieved through a uniaxial shear tester [42], where the diameter of the specimen was 150 mm and the height 50 mm, with a hollow diameter of 50 mm. During the test, the specimen is placed in a steel mold, which limits the lateral deformation of the specimen. This is similar to apply a confining pressure on the specimen. A vertical axle load is also applied to simulate the shearing action on the asphalt mixtures.

2.4. Uniaxial Penetration Test. The uniaxial penetration test method was proposed by Tongji University [43], and the idea came from the California bearing rate (CBR) test in the geotechnical test method. The test uses a cylindrical steel rod to apply load on the asphalt mixture specimen to simulate actual pavement stress, but this method does not directly measure the shear strength of the specimen and needs to be combined with the unconfined compression test to determine the C and φ values of the asphalt mixture, which increases the difficulty and complexity of the operation. The *Specifications for Design of Highway Asphalt Pavement* (JTG D50-2017) of China proposed the use of the uniaxial penetration test to check the penetration strength of an asphalt mixture to control permanent deformation in an asphalt mixture. Although the method was simple to operate, some studies found that the specimen did not show an obvious shear failure surface after the test was completed [44], and others felt that further study is needed for the material property assumptions, stress conditions, and mechanical models of this method [45].

In summary, each of the above test methods had their own particular advantages and disadvantages and also required special sophisticated equipment, making these tests difficult to put into practical for asphalt mixture design and field quality control. Thus, it is important to further research and develop shear test methods.

3. Objectives

In order to evaluate the shear performance of an asphalt mixture in a practical manner, the paper proposes a torsional test method under normal stress condition [46]. Preliminary testing indicated that the method had the following characteristics:

(i) The physical concept and principles of the method were clear, test results were stable, and there was good reproducibility

(ii) The method was convenient for operation, the specimen fabrication was simple, the method also had the capacity to test cores obtained from the existing pavement, and it was compatible with equipment currently available in materials laboratories

(iii) The results showed that shear strength increased with an increase of normal stress and presented a

linear relation, which satisfied the Mohr–Coulomb strength theory; thus, the principle of the experiment was correct

However, the method had the following shortcomings: first, there were only two types of asphalt mixture utilized for verification, and thus representativeness was limited. Second, changes in the height of the specimen under normal stress during the test were not investigated. A change of height means that the volume of the specimen changes, which will result in inaccurate test results. Third, the linear regression method was used to determine the cohesion C and the internal friction angle φ, which does not meet the Mohr–Coulomb strength mechanics principle.

Therefore, in order to further analyze the feasibility and reliability of the method, the objective of this study is as follows:

(i) Analyze specimen stress characteristics of the torsional test method under normal stress condition, and obtain the calculation formula for shear strength

(ii) Based on Mohr–Coulomb theory, obtain a method for calculating the cohesion and the internal friction angle

(iii) Analyze volume change of the specimen during the test, and analyze the damage characteristics of the specimen

(iv) Study and evaluate the impact of asphalt mixture types and test temperature on shear performance

(v) Perform a torsional fatigue test to obtain q torsion shear fatigue model

4. Torsional Test under Normal Stress

The basic principle of the torsional test method under normal stress condition is that normal stress is uniformly applied to the specimen by the jack and the magnitude of the normal stress is measured by the load cell. The vertical load of the material test system (MTS) was converted into torque by the rack and the gear, so the asphalt mixture cylindrical specimen is in a state of compression and shear. With an increase of torque, the shear stress exceeds the shear strength of the asphalt material itself, and a crack occurs, with the specimen gradually destroyed [32]. Based on the Mohr–Coulomb strength theory, it is possible to obtain shear strength, cohesion C, and internal friction angle φ of the asphalt mixture.

The test device consists of a universal material testing machine and a shear test platform. The universal material test system (CMT5105) includes an incubator, loading frame, control system, power system, data acquisition system, and other components to control loading frequency, loading magnitude, and loading cycles and also to collect parameters such as load and vertical displacement in real time.

The shear test platform is shown in Figure 1 and consists of a baffle (1), a joint (2), a rack (3), and a gear (4) (36 teeth in total, with a pitch of 18.85 mm, and each tooth corresponds to a twist of 10°), a coupling (5), torque sensor (6), angle sensor (7), wire drawing displacement sensor (8), load cell (9), jack (10), fixed side pressure plate (11), sliding dovetail groove and baffle (12), fixed base (13), and round rod (14). The test device could be seen in Figure 2 in the literature [32].

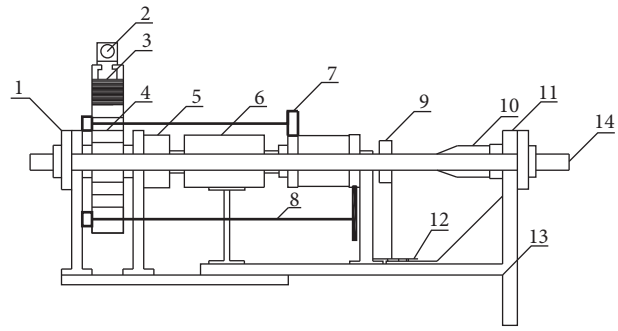

Figure 1: The shear test platform.

Based on the equipment, a torque sensor (6), angle sensor (7), and wire drawing displacement sensor (8) were added to ensure the accuracy of data acquisition. Torque was measured by the torque sensor (6) (range 0–±100 kN·m), while angular displacement was determined by the angle sensor (7) during torsional deformation of the specimen. The wire drawing displacement sensor (8) and the specimen were connected by using screws to the fixed end of the plate such that the height of the specimen could be measured during the test.

5. Mechanical Analysis of Torsional Test under Normal Stress Condition

Four basic rules were assumed:

(i) The asphalt mixture specimen was ideally elastic, completely uniform, and isotropic

(ii) Internally, the specimen had continuity, regardless of the atomic structure of the substance and its molecular motion

(iii) The initial stress that existed in the specimen was equal to zero before the load was applied

(iv) When the specimen was loaded, the displacement of each point was much smaller than the size of the specimen, and the rotation angle and deformation were much less than 1

5.1. Analysis of Shear Stress. To analyze the torsional force on the cylindrical specimen, origin point O of the rectangular coordinate system was placed on the left end centroid. The bus bar of the cylinder extends to the right and was parallel to the z-axis. The main axis of the section coincides with the x-axis and the y-axis, and the z-axis constitutes the right-handed system, as shown in Figure 2.

When the specimen was twisted, the relaxation boundary condition at the $z = l$ end was as follows:

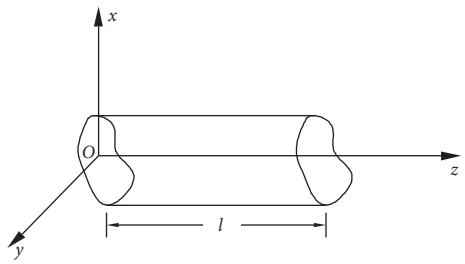

Figure 2: Schematic diagram of the cylindrical specimen.

$$\begin{cases} \iint_G \tau_{zx}\mathrm{d}x\mathrm{d}y = \iint_G \tau_{zy}\mathrm{d}x\mathrm{d}y = \iint_G \sigma_z\mathrm{d}x\mathrm{d}y = 0, \\ \iint_G y\sigma_z\mathrm{d}x\mathrm{d}y = \iint_G x\sigma_z\mathrm{d}x\mathrm{d}y = 0, \\ \iint_G \left(x\tau_{zy} - y\tau_{zx}\right)\mathrm{d}x\mathrm{d}y = M_z. \end{cases} \tag{1}$$

Assuming $\sigma_x = \sigma_y = \sigma_z = \tau_{xy} = 0$, the torsional stress function was determined by the boundary equation of the circular section as

$$\phi = m\left(\frac{x^2 + y^2}{r^2} - 1\right). \tag{2}$$

This could be obtained by the intradomain equation:

$$\nabla^2\phi = \frac{\partial^2\phi}{\partial x^2} + \frac{\partial^2\phi}{\partial y^2} = 2m + 2m = 4m = -2G\,\partial. \tag{3}$$

Solve $m = -(G\,\partial r^2/2)$, obtained from the torsional formula:

$$M_z = 2\iint \phi\mathrm{d}x\mathrm{d}y = 2m\iint\left(\frac{x^2 + y^2}{r^2} - 1\right)\mathrm{d}x\mathrm{d}y. \tag{4}$$

According to the nature of the circular section, the integral was $M_z = -m\pi r^2$, and simultaneous (2)–(4) solutions were obtained:

$$\tau = \sqrt{\tau_{zx}^2 + \tau_{zy}^2} = \frac{2M_z}{\pi r^4}\sqrt{x^2 + y^2}. \tag{5}$$

Thus, the torsional shear stress was linearly distributed and the maximum shear stress occurred at the boundary point and was $\tau_{\max} = (2M_z/\pi r^3) = (2T/\pi r^3)$.

5.2. Determination of Shear Strength Parameters for Asphalt Mixtures. A microelement body was taken from the specimen, and it was assumed that the stress on each surface of the microelement body was uniform and that the stresses on the front and back sides were 0, which could be converted into a plane problem, as shown in Figure 3.

From the microelement body stress balance property, the balance equation was

$$\begin{aligned} \sum F_x &= 0, \\ \sum M_z &= 0, \end{aligned} \tag{6}$$

where $\tau\mathrm{d}z\mathrm{d}y = \tau'\mathrm{d}x\mathrm{d}z$ and $\tau\mathrm{d}z\mathrm{d}y\mathrm{d}x = \tau'\mathrm{d}x\mathrm{d}z\mathrm{d}y$; after simplification, $\tau = \tau_0'$ could be obtained.

Take any oblique section *ef* perpendicular to the front and back planes in the microelement body, as shown in Figure 4.

From the stress balance equation $\sum F_\eta = 0$ and $\sum F_\xi = 0$ of the separation body, the solution was

$$\begin{aligned} &-\sigma_a\mathrm{d}A + (\tau_x\mathrm{d}A\cos a)\sin a + (\sigma_x\mathrm{d}A\cos a)\cos a \\ &\quad + (\tau_z\mathrm{d}A\sin a)\cos a = 0, \end{aligned} \tag{7}$$

$$\begin{aligned} &\tau_a\mathrm{d}A - (\tau_x\mathrm{d}A\cos a)\cos a + (\sigma_x\mathrm{d}A\cos a)\sin a \\ &\quad + (\tau_z\mathrm{d}A\sin a)\sin a = 0. \end{aligned} \tag{8}$$

According to the principle of shear stress mutual equality, the values of τ_x and τ_z were equal, and the simultaneous (7) and (8) solutions were obtained:

$$\left(\sigma_a - \frac{\sigma_x}{2}\right)^2 + \tau_a^2 = \left(\frac{\sigma_x}{2}\right)^2 + \tau_x^2. \tag{9}$$

From the above equation, the center point of the circle was on the abscissa (σ-axis), the abscissa was $(\sigma_x/2)$, and the radius was $\sqrt{(\sigma_x/2)^2 + \tau_x^2}$, as shown in Figure 5.

The radius $\overline{CD_1}$ of the stress circle was rotated from α to 2α, and a radius $\overline{CE}$ was obtained, as shown in Figure 6. The ordinates of A_1 and A_2 were 0, and the abscissa was the principal stresses σ_1 and σ_3, respectively. The abscissas of A_1 and A_2 were

$$\begin{aligned} \overline{OA_1} &= \overline{OC} + \overline{CA_1}, \\ \overline{OA_2} &= \overline{CA_2} - \overline{OC}, \end{aligned} \tag{10}$$

where $\overline{OC}$ was the abscissa of the center of the stress circle and $\overline{CA_1}$ was the radius of the stress circle.

The principal stress values could be calculated from equation (3) in the literature [32].

The failure criterion of the asphalt mixture can be expressed by the large and small principal stresses, with the following total stress formula:

$$\frac{(\sigma_1 - \sigma_3)_f}{2} = \frac{(\sigma_1 + \sigma_3)_f}{2}\sin\varphi + c\cos\varphi, \tag{11}$$

where $((\sigma_1 - \sigma_3)_f/2)$ and $((\sigma_1 + \sigma_3)_f/2)$ are the coordinates of the limit total stress circle point at the time of specimen failure.

The intensity envelope curve was approximately a straight line, and the envelope curve parameter can be represented by a constant. Through equation (9), an approximate straight line (k_f line) was obtained by regression analysis. Since the intersection of the intensity envelope curve and the horizontal axis of the coordinate can be regarded as a point circle in the limit equilibrium state, the k_f line must also intersect the horizontal axis at that point, as shown in Figure 3 in the literature [32].

Assuming that the inclination of the k_f line was α_f and the intercept of the horizontal axis of the coordinate was d_f, the following equation can be obtained:

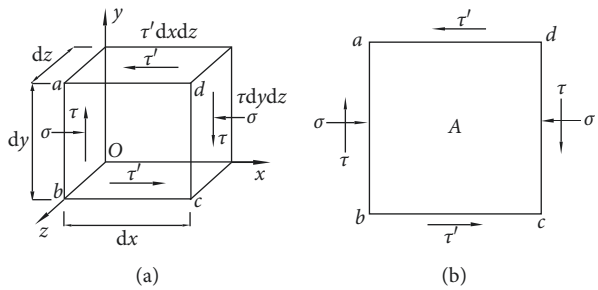

Figure 3: Schematic diagram of the stress state of the microelement body.

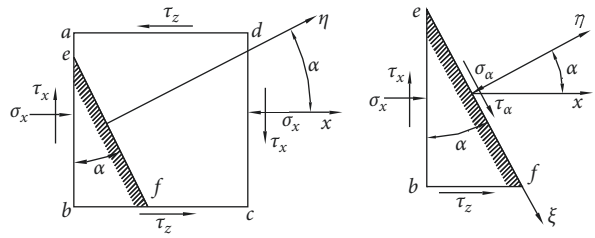

Figure 4: Schematic diagram of the stress state of the oblique section of the microelement body.

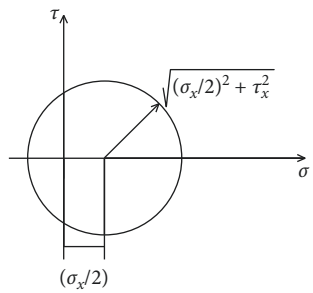

Figure 5: Stress Mohr circle.

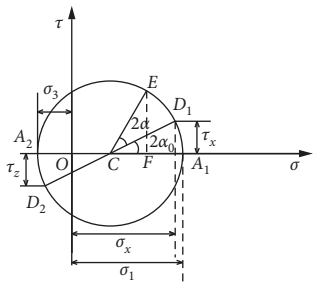

Figure 6: Stress Mohr circle after rotating 2α angle.

$$\tan \alpha_f = \sin \varphi, \tag{12}$$

$$d_f = c * \cos \varphi. \tag{13}$$

Therefore, when the k_f line is known, then α_f and d_f are known, and the strength parameters of the asphalt mixture can be calculated according to equations (12) and (13).

Based on Mohr–Coulomb theory, torsional shear strength tests were done under different normal stresses, and the Mohr–Coulomb failure envelope curve was calculated. The envelope curve was defined as

$$\tau = c + \sigma \tan \varphi, \tag{14}$$

where τ was the shear stress, σ was the normal stress, c was the cohesion, φ was the internal friction angle, and $\tan\varphi$ was the slope of the failure envelope curve.

Since the strength envelope line of the asphalt mixture could not be obtained by a Mohr circle, the torsional shear test was done for at least three different normal stresses in order to calculate the principal stresses σ_1 and σ_3 values and to derive the common envelope curve of each Mohr circle.

In Figure 3 in the literature [32], the dashed line is the k_f line, and the k_f line passes through the maximum shear stress of each failed Mohr circle. Then, p and q can be used to determine the coordinates of the maximum shear stress. p and q are determined by formula (15), then the k_f line is obtained by linear regression method, and intercept a_0 and angle α were determined from the ordinate. The C and φ values of the mixture can be obtained according to formula (16):

$$p = \frac{(\sigma_1 + \sigma_3)}{2},$$
$$q = \frac{(\sigma_1 - \sigma_3)}{2}, \tag{15}$$

$$\varphi = \sin^{-1}(\tan \alpha),$$
$$c = \frac{a_0}{\cos \varphi}. \tag{16}$$

6. Experimental Program

6.1. Materials. Torsional testing was done using four types of asphalt mixture, which are commonly used in China: SMA-13, AC-13, AC-20, and AC-25.

The unmodified asphalt of #A-70 was used for an asphalt mixture, and the relevant properties of asphalt including penetration, ductility, softening point, and density, etc., were tested according to the *Chinese Standard Test Method for Asphalt and Asphalt Mixture for Highway Engineering* (JTG E20-2011), and the results meet the requirements of the specification.

Limestone was selected for the aggregate, and the filler was obtained by using milled limestone powder. The Los Angeles abrasion loss, polishing value, density, flat and elongated particles content, adhesion, angularity, sand equivalent, etc., were tested in accordance with the requirements of the *Chinese Test Method of Aggregate for Highway Engineering* (JTG E42-2005), and the test results meet the requirements of the specification.

6.2. Mix Design. The gradations of four types of asphalt mixture are shown in Figure 7.

The Marshall method was used for the mixture design, and optimal asphalt aggregate ratio and related volume parameters were obtained as shown in Table 1.

6.3. Specimen Preparation. The specimen was formed by a gyratory compactor with a size of Φ100 mm × 100 mm. After the specimen is extruded, the height in five different positions was tested by a Vernier caliper, and the difference was not more than 2 mm. The specimens are shown in Figure 8.

6.4. Testing Conditions. A temperature of 60°C was selected as the test temperature, the loading rate was 1 mm/min, and the normal stress was 0.7 MPa (Chinese standard axle tire pressure). Torsional shear testing was done on the four types of asphalt mixture to study variations in shear strength and shear modulus of the asphalt mixtures.

In addition, in order to study the distribution law of C and φ of asphalt mixtures, two kinds of asphalt mixture, AC-13 and AC-20, were selected for testing, the test temperature was 60°C, and the normal stress levels of the torsional test were 0 MPa, 0.35 MPa and 0.7 MPa.

7. Results and Analysis

7.1. Failure Mode of Specimens. The specimens after destruction are shown in Figure 9.

The failure position of the specimens is shown in Figure 9. Observation of this failure shows that a small crack appears near the loading end and then as the load increases, the crack gradually extends to form an oblique crack at about 45° from the vertical axis. At the same time, there was bulging around the specimen until the specimen was completely destroyed. The failure mode of the specimen accords with shear failure characteristics.

The relationship between torque, torsional angle, and time was measured by the torque sensor and the angle sensor, as shown in Figure 10 (using the asphalt mixture of the AC-13 specimen as an example).

Figure 10 shows that as loading progressed, the torque gradually increased with time, reached a maximum value at a certain moment, and then decreased, which was the maximum torque that the specimen could bear at that time, then the specimen was damaged, and the corresponding shear strength of the asphalt mixture could be obtained.

At the same time, the torsional angle increased with time and reflected how the shear strain of the specimen increased until the specimen was destroyed. The strain value corresponding to the maximum torque was the shear strain of destruction for the specimen.

In addition, according to the results from the wire drawing displacement sensor, the displacement was very small, about 0.03 mm, which reflected the change in the height direction of the specimen. This showed that the height of the specimen was basically constant during the experimental process, and the volume of the specimen did not change, which ensured the accuracy and reliability of the test results.

7.2. Influence of Asphalt Mixture Type. Four parallel tests were done to obtain the shear strength and shear modulus of different asphalt mixtures, as shown in Figure 11.

The results show that the "error bar" for the four asphalt mixtures was small, and the coefficient of variation ranged from 5.0% to 8.6%, demonstrating acceptable repeatability of the torsional test.

The asphalt mixture consisted of asphalt and mineral aggregate, and shear strength was derived from bonding of the asphalt binder and the interlock of the aggregate gradation [29]. For the asphalt mixture of AC, as the nominal maximum aggregate size increased, shear strength decreased and shear modulus decreased, which was consistent with the actual situation. Because the AC asphalt mixture was a "suspension-dense" structure, the interlock of aggregates in three different nominal particle sizes was limited. When the nominal maximum aggregate size was small, the content of fine aggregate in the mixture was relatively large such that the specific surface area of the aggregate increased, resulting in an increase in the amount of asphalt and an increase in the proportion of structural asphalt such that the bonding effect of the mortar increased and also the shear strength of the asphalt mixture increased.

The shear strength and modulus of the SMA-13 asphalt mixture were larger than those of the AC-13 asphalt mixture. The gradation of SMA-13 was a "gap-graded" type, and within this type of mixture, the content of coarse aggregate was more than 70%, thus providing a better interlock action among the coarse aggregates. Thus, the shear performance of SMA-13 was better than that of AC-13.

7.3. Influence of Temperature. Torsional testing for the asphalt mixture of AC-13 was performed at five temperatures: 20°C, 30°C, 40°C, 50°C, and 60°C. The specimen was held in an environmental chamber for 4 to 6 hours, with a normal

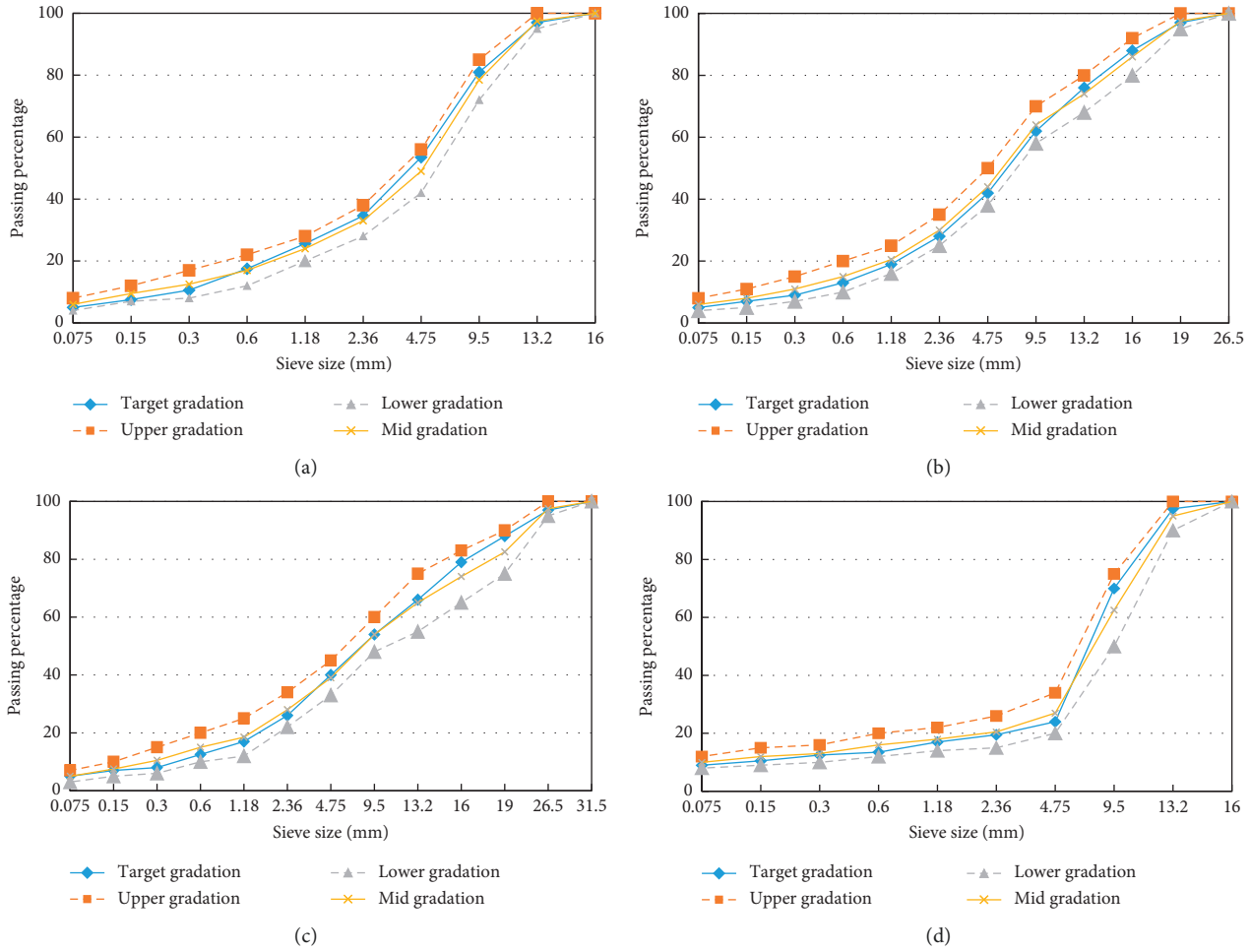

Figure 7: Gradations of four types of asphalt mixture. (a) AC-13, (b) AC-20, (c) AC-25, and (d) SMA-13.

Table 1: Summary of volumetric parameters of asphalt mixtures.

Mixture type	Optimal asphalt aggregate ratio (%)	Bulk density (g/cm^3)	Stability (kN)	Flow value (mm)	Air voids (%)	VMA (%)	VFA (%)
AC-13	4.9	2.416	13.8	3.04	4.8	14.6	68.4
AC-20	4.5	2.448	15.12	2.78	4.0	13.2	70.6
AC-25	4.0	2.441	14.8	3.37	5.1	13.4	62.8
SMA-13	6.3	2.377	6.28	4.83	3.47	17.8	80.7

Figure 8: Asphalt mixture specimen. (a) AC-13; (b) AC-20; (c) AC-25; (d) SMA-13.

(a) (b) (c) (d)

Figure 9: Specimens after destruction. (a) AC-13; (b) AC-20; (c) AC-25; (d) SMA-13.

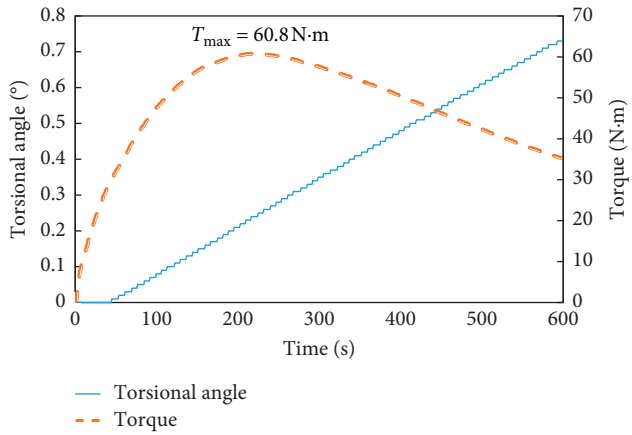

Figure 10: Torque and torsional angle versus time (AC-13).

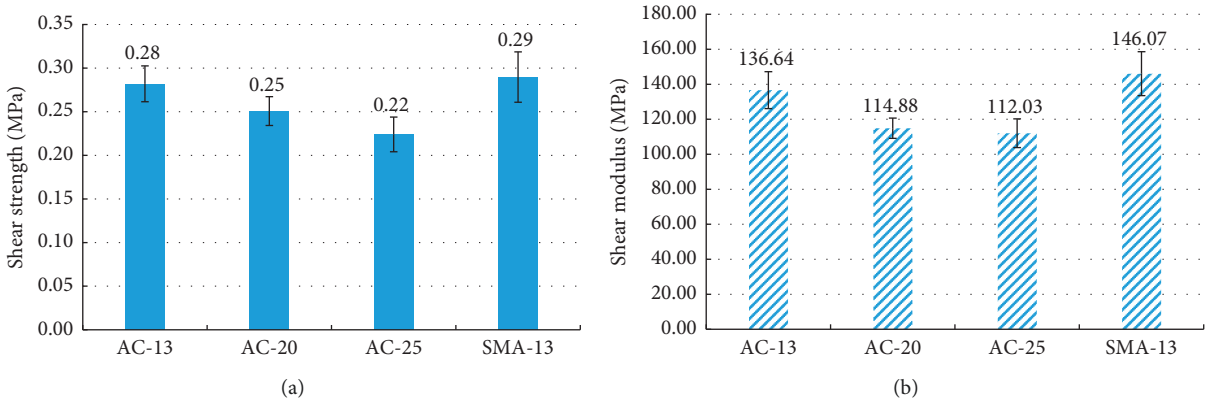

Figure 11: (a) Shear strength and (b) shear modulus of asphalt mixtures.

stress of 0.7 MPa and loading speed of 1 mm/min, and the parallel test was repeated four times. The results are shown in Figure 12.

As temperature increased, the shear strength and shear modulus of the asphalt mixture decreased, and shear strength decreases by about 0.1 to 0.2 MPa for every 10°C increase in temperature. As the asphalt mixture was a typical viscoelastic material, the asphalt gradually softened with an increase of temperature, and the cohesion between the asphalt and the mineral material decreased. Shearing resistance mainly relied on the interlock between the aggregate particles, which resulted in a reduction in the shear strength of the asphalt mixture. The test results reflect the influence of temperature on the shear performance of asphalt mixture,

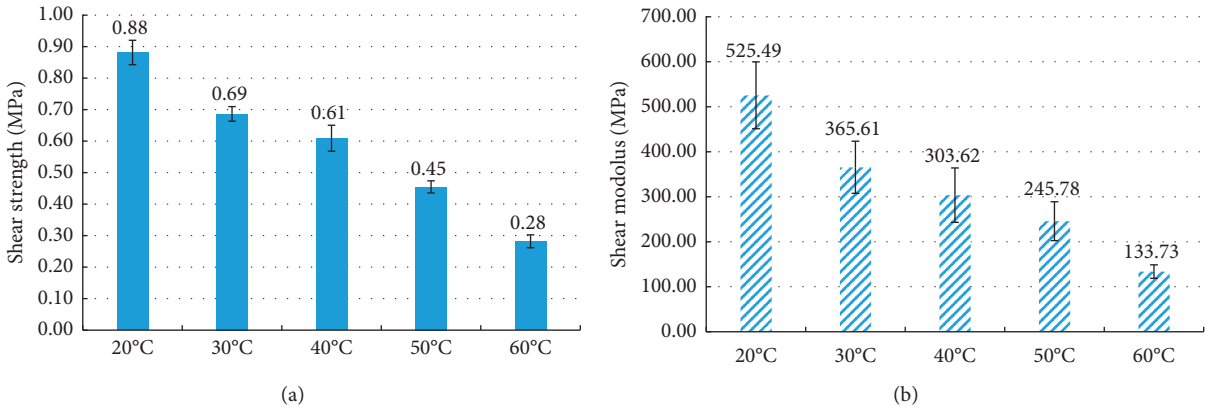

Figure 12: (a) Shear strength and (b) shear modulus at different temperatures.

which accords with findings in the field. Reasonable test results were obtained from this method.

7.4. Shear Strength Parameters. Torsional test results at a temperature of 60°C for asphalt mixtures of AC-13 and AC-20 are shown in Figure 13, with the normal stress levels during the torsional test at 0 MPa, 0.35 MPa, and 0.7 MPa, with a parallel test repeated three times.

The cohesion of AC-13 was larger than that of AC-20, but the internal friction angle was smaller than AC-20. This was because when the maximum nominal particle size was small, the content of fine aggregate in the mixture was relatively high, and the amount of asphalt increased, thus the proportion of structural asphalt increased, resulting in an increase in the contact area between the aggregate and the asphalt, and thus cohesion also increased. As the maximum nominal particle size increases, the content of the coarse aggregate in the mixture increases, and the possibility that the coarse aggregates come into contact with each other to form the interlock increases, resulting in an increase of the internal friction angle, which is consistent with the results of the literature [32].

A torsional test for the AC-13 asphalt mixture was done at three different temperatures, 20°C, 40°C, and 60°C, and the normal stress levels of the torsional test were 0 MPa, 0.35 MPa, and 0.7 MPa, with the parallel test repeated three times. Results are shown in Figure 14.

As the temperature increased, the cohesion C decreased. When the temperature exceeded 40°C, the values of C clearly decreased. Thus, due to the viscoelastic properties of the asphalt mixture, temperature had a significant effect on shear properties. After the temperature increased, the asphalt softened, resulting in decreased cohesion. At the same time, the softened asphalt also played a role in intrusion of the aggregate, resulting in a decrease of the internal friction angle. Therefore, the higher the temperature, the worse the shear performance of the asphalt mixture.

As shown in Figure 14, the internal friction angle φ was basically equivalent under three different temperatures, also showing slight deviation, which indicates that the temperature changes had little effect on the value of the internal friction angle. The internal friction angle of the mixture was determined by the mutual interlock of the aggregates and was mainly related to the spatial distribution of the aggregate gradation of the mixture itself, and as such external conditions such as temperature had little effect on it, which is also consistent with the results of the literature [32].

In the summer with high temperatures, the surface temperature of asphalt pavement can reach above 50~60°C, which leads to a rapid decrease of C values in the asphalt mixture, and which is also the inherent reason for the rutting deformation found in asphalt pavement.

8. Torsional Fatigue Test

In a pavement structure, a single load application is unlikely to cause shear failure, but asphalt pavement rutting and surface cracking can occur due to repeated loading. Therefore, it is important to investigate the behavior of shear fatigue under repeated loading conditions.

An AC-13 asphalt mixture was used for torsional fatigue testing. The loading frequency was 10 Hz, with a sinusoidal waveform load with no intermittent time. As fatigue usually occurred at intermediate temperatures rather than high temperatures, the test temperature was set at 20°C, and the test was done at four shear stress levels of 0.4, 0.5, 0.6, and 0.7, and the number of loading times when the specimen was completely destroyed was taken as the fatigue life. Test results are shown in Figure 15.

The number of replicates for a fatigue test is 4, and the results of Figure 15 are the average values after abnormal data were discarded according to the methods of Grubbs's criterion for suspicious data selection.

Under the same normal stress condition, the fatigue life of an asphalt mixture decreased along with the increase of shear stress level. The higher the stress level, the shorter the fatigue life of the asphalt mixture, which indicated that the asphalt pavement was more prone to shear fatigue failure under overload conditions. In addition, shear fatigue life at a normal stress of 0.7 MPa was larger than shear fatigue life at a normal stress of 0.5 MPa.

Studies have shown that the fatigue life and stress levels of asphalt mixtures exhibit a linear relationship on a single logarithmic coordinate system. Fatigue life and shear stress levels were plotted on logarithmic coordinates and fitted as shown in Figure 16.

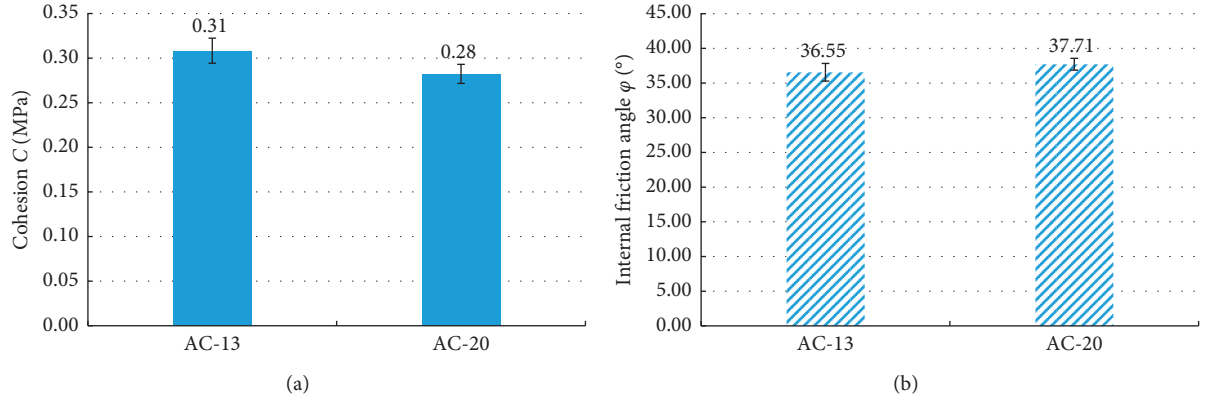

Figure 13: (a) C and (b) φ test results of asphalt mixture.

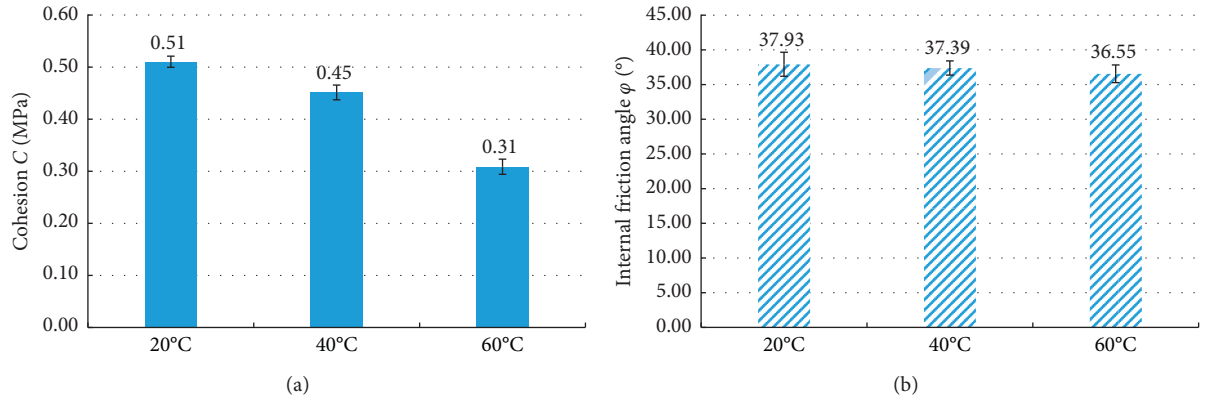

Figure 14: Test results of (a) C and (b) φ at different temperatures.

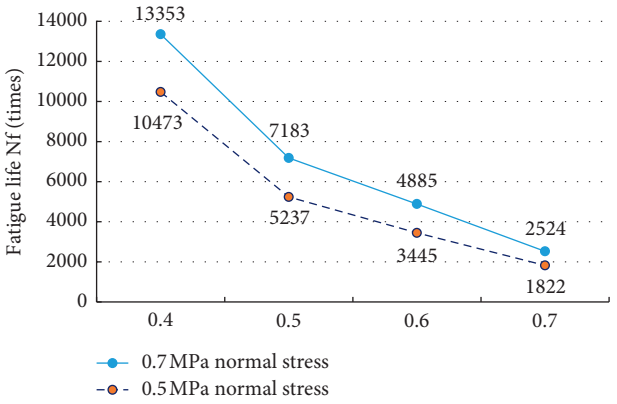

Figure 15: Relationship between fatigue life and shear stress ratio.

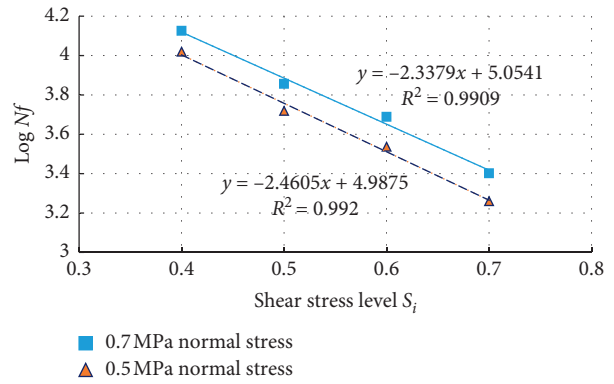

Figure 16: Log (N_f) curve of the AC-13 shear fatigue test.

The regression variants (R^2) from the shear fatigue envelope, which varied from 0.991 to 0.992, had a high correlation. The shear fatigue equation was applied to two scenarios:

$$\begin{aligned} \lg N_f &= 5.0541 - 2.3379S_i \quad \text{normal stress } 0.7 \text{ MPa}, \\ \lg N_f &= 4.9875 - 2.4605S_i \quad \text{normal stress } 0.5 \text{ MPa}, \end{aligned} \tag{17}$$

where S_i was the shear stress level.

In order to speed up the test progress, in this experiment the no-interval time for the loading mode was selected, but the actual traffic load on pavement is different, and a certain point on the surface of the pavement structure would not be continuously affected by the traffic load. Therefore, under an intermittent traffic load, due to the viscoelastic properties of the asphalt mixture, fine cracks would gradually heal, which would led to an increase in actual pavement fatigue life. Therefore, when applied to the laboratory model to

investigate actual pavement fatigue life, it is also necessary to consider the impact of intermittent time of the load and apply a field correction.

9. Conclusions and Recommendations

In this paper, four asphalt mixtures were selected for torsional testing under normal stress condition at different temperature conditions. The following conclusions can be summarized from this study and laboratory investigation:

(i) During the torsional test, the height and the volume of the specimen were kept basically constant, which ensured the accuracy and reliability of the shear test results.

(ii) There was an oblique crack at about 45° from the vertical axis of the specimen that occurred after the specimen was destroyed, and the failure mode of the specimen accorded with shear failure characteristics.

(iii) Through mechanical analysis, the calculation formulas for shear strength and shear parameters (cohesion and internal friction angle) of the torsional test under normal stress condition were obtained.

(iv) The torsional test method provided repeatable results for shear resistance of asphalt mixtures at different temperatures.

(v) For the AC asphalt mixture type, as the maximum nominal particle size increased, shear strength and shear modulus decreased. In addition, the shear strength and shear modulus of the SMA-13 asphalt mixture were larger than those of the AC-13 asphalt mixture. The test results reflect the difference in shear performance of different types of asphalt mixture.

(vi) As the temperature increased, shear strength and shear modulus of the asphalt mixture decreased, and the test results reflected the influence of temperature on the shear performance of the asphalt mixture, which accorded with findings in the field.

(vii) For the AC-type asphalt mixture, as the maximum nominal particle size increased, the cohesion C decreased and the internal friction angle φ increased, reflecting the influence of the internal asphalt mixture structure on shear parameters. At the same time, as temperature increased, the cohesion C decreased. When the temperature exceeded 40°C, the values of C clearly decreased, which could explain the mechanism of rutting deformation in asphalt pavement.

(viii) Internal friction angle φ was basically equivalent under three different temperatures, which indicates that temperature change had little effect on the value of the internal friction angle, which was mainly related to spatial distribution and the mutual interlock of the aggregates gradation of the mixture.

(ix) Fatigue life decreased with increasing shear stress levels, and thus a shear fatigue model was obtained.

(x) Torsional test method under normal stress formed a compression-shear action on the specimen by applying torque and normal stress, compared with direct shear test, thus simulating the vertical loads of vehicles applying normal stress. The proposed torsional test method under normal stress can evaluate the shear performance of asphalt mixtures.

Data Availability

The data used to support the findings of this study are included within the article.

Conflicts of Interest

The authors declare no conflicts of interest.

Acknowledgments

The authors would like to acknowledge the financial support of the National Natural Science Foundation of China (Grant no. 51978083) and China Scholarship Council (Grant no. 201808430101).

References

[1] A. Hofstra and A. J. G. Klomp, "Permanent deformation of flexible pavements under simulated road traffic conditions," in *Proceedings of the 3rd International Conference on the Structural Design of Asphalt Pavements*, vol. 1, pp. 613–621, London, UK, September 1972.

[2] J. Eisenmann and A. Hilmer, "Influence of wheel load and inflation pressure on the rutting effect at asphalt pavements-experiments and theoretical investigations," in *Proceedings of the 6th International Conference on the Structural Design of Asphalt Pavements*, vol. 1, pp. 392–403, University of Michigan, Ann Arbor, MI, USA, July 1987.

[3] J. B. Sousa, C. Joseph, and C. L. Monismith, *Summary Report on Permanent Deformation in Asphalt Concrete*, Strategic Highway Research Program, National Research Council, Washington, DC, USA, 1991.

[4] A. H. Gerritsen, C. A. P. M. Van Gurp, J. P. J. van der Heide, A. A. A. Molenaar, and A. C. Pronk, "Prediction and prevention of surface cracking in asphaltic pavements," in *Proceedings of the 6th International Conference on the Structural Design of Asphalt Pavements*, vol. 1, pp. 378–391, University of Michigan, Ann Arbor, MI, USA, July 1987.

[5] S. Matsuno and T. Nishizawa, "Mechanism of longitudinal surface cracking in asphalt pavement," in *Proceedings of the 7th International Conference on the Structural Design of Asphalt Pavements*, Nottingham, UK, 1992.

[6] J. S. Uhlmeyer, K. Willoughby, L. M. Pierce, and J. P. Mahoney, "Top-down cracking in Washington state asphalt concrete wearing courses," *Transportation Research Record: Journal of the Transportation Research Board*, vol. 1730, no. 1, pp. 110–116, 2000.

[7] E. Freitas, P. Pereira, and L. Picado-Santos, "Assessment of top-down cracking causes in asphalt pavements," in *Proceedings of the 3rd International Symposium on Maintenance and Rehabilitation of Pavements and Technological Control*, pp. 555–564, Guimarães, Portugal, 2003.

[8] E. Freitas, P. Pereira, L. Picado-Santos, and A. Thomas Papagiannakis, "Effect of construction quality, temperature, and rutting on initiation of top-down cracking," *Transportation Research Record: Journal of the Transportation Research Board*, vol. 1929, pp. 174–182, 2005.

[9] A. A. A. Molenaar, "Fatigue and reflective cracking due to traffic (with discussion)," *Proceedings of the Association of Asphalt Paving Technologists*, vol. 53, pp. 440–474, 1984.

[10] L. A. Myers, R. Roque, and B. E. Ruth, "Mechanisms of surface-initiated longitudinal wheel path cracks in high-type bituminous pavements," *Proceedings of the Association of Asphalt Paving Technologists*, vol. 67, pp. 401–432, 1998.

[11] L. A. Myers, R. Roque, and B. Birgisson, "Propagation mechanisms for surface-initiated longitudinal wheel path cracks," *Transportation Research Record: Journal of the Transportation Research Board*, vol. 1778, no. 1, pp. 113–121, 2001.

[12] T. Svasdisant, M. Schorsch, B. Gilbert, and S. Pinyosunun, "Mechanistic analysis of top-down cracks in asphalt pavements," *Transportation Research Record: Journal of the Transportation Research Board*, vol. 1809, no. 1, pp. 126–136, 2002.

[13] J. Groenendijk, *Accelerated testing and surface cracking of asphaltic concrete pavements*, Ph.D. thesis, Delft University of Technology, Delft, Netherlands, 1998.

[14] A. Bensalem, A. J. Broen, M. E. Nunn, D. B. Merrill, and W. G. Lloyd, "Finite element modeling of fully flexible pavements: surface cracking and wheel interaction," in *Proceedings of the 2nd International Symposium on 3D Finite Element for Pavement Analysis, Design, and Research*, pp. 103–121, Charleston, WV, USA, October 2000.

[15] L. Sun and F. Li, "Finite element analysis of top-down cracking in asphalt pavement," *Journal of Highway and Transportation Research and Development*, vol. 23, no. 6, pp. 1–4, 2006, in Chinese.

[16] H. Wang and I. L. Al-Qadi, "Evaluation of surface-related pavement damage due to tire braking," *Road Materials and Pavement Design*, vol. 11, no. 1, pp. 101–121, 2010.

[17] F. Gu, W. Ma, R. C. West, A. J. Taylor, and Y. Zhang, "Structural performance and sustainability assessment of cold central-plant and in-place recycled asphalt pavements: a case study," *Journal of Cleaner Production*, vol. 208, pp. 1513–1523, 2019.

[18] D. W. Christensen, R. Bonaquist, and D. P. Jack, "Evaluation of triaxial strength as a simple test for asphalt concrete rut resistance," Final report, Pennsylvania State University, State College, PA, USA, 2000.

[19] P. Jaskuła, "Influence of compaction effectiveness on interlayer bonding of asphalt layers," in *Proceedings of the 9th International Conference "Environmental Engineering 2014"*, Vilnius, Lithuania, May 2014.

[20] G. A. Sholar, G. C. Page, J. A. Musselman, P. B. Upshaw, and H. L. Moseley, "Preliminary investigation of a test method to evaluate bond strength of bituminous tack coats," *Journal of the Association of Asphalt Paving Technologists*, vol. 73, pp. 771–806, 2004.

[21] O. Vacin, J. Ponniah, and S. Tighe, "Quantifying the shear strength at the asphalt interface," in *Proceedings of the 1st Annual International University Symposium on Infrastructure Management (AISIM)*, University of Waterloo, Waterloo, Canada, August 2005.

[22] M. Diakhate, A. Phelipot, A. Millien, and C. Petit, "Shear fatigue behaviour of tack coats in pavements," *Road Materials and Pavement Design*, vol. 7, no. 2, pp. 201–222, 2006.

[23] F. Canestrari, G. Ferrotti, M. Partl, and E. Santagata, "Advanced testing and characterization of interlayer shear resistance," *Transportation Research Record: Journal of the Transportation Research Board*, vol. 1929, no. 1, pp. 69–78, 2005.

[24] I. L. Al-Qadi, S. H. Carpenter, Z. Leng et al., *Tack Coat Optimization for HMA Overlays: Laboratory Testing*, Illinois Center for Transportation, Rantoul, IL, USA, 2008.

[25] L. N. Mohammad, A. Bae, M. A. Elseifi, J. Button, and J. A. Scherocman, "Interface shear strength characteristics of emulsified tack coats," *Journal of the Association of Asphalt Paving Technologists*, vol. 78, pp. 249–279, 2009.

[26] R. C. West, J. Zhang, and J. Moore, "Evaluation of bond strength between pavement layers," NCAT Report 05-08, National Center for Asphalt Technology, Auburn, AL, USA, 2005.

[27] M. R. Kruntcheva, A. C. Collop, and N. H. Thom, "Properties of asphalt concrete layer interfaces," *Journal of Materials in Civil Engineering*, vol. 18, no. 3, pp. 467–471, 2006.

[28] D. W. Christensen Jr, R. F. Bonaquist, and T. Handojo, "Field shear test device for quality control testing of asphalt concrete," *Journal of the Association of Asphalt Paving Technologists*, vol. 71, pp. 386–416, 2002.

[29] M. Guler, H. U. Bahia, P. J. Bosscher, and M. E. Plesha, "Device for measuring shear resistance of hot-mix asphalt in gyratory compactor," *Transportation Research Record: Journal of the Transportation Research Board*, vol. 1723, no. 1, pp. 116–124, 2000.

[30] W. H. Goetz and J. H. Schaub, "Triaxial testing of bituminous mixtures," in *Bituminous Paving Materials*, pp. 51–63, ASTM International, West Conshohocken, PA, USA, 1959.

[31] C. L. Monismith and A. A. Tayebali, "Permanent deformation (rutting) considerations in asphalt concrete pavement sections," *Proceedings of the Association of Asphalt Paving Technologists*, vol. 57, pp. 414–463, 1988.

[32] J. Xie and Y. Wang, "Comparative study on torsional shear and triaxial test of asphalt mixtures," *Advances in Civil Engineering*, vol. 2019, Article ID 1856298, 8 pages, 2019.

[33] S. F. Brown, "Improved framework for predicting permanent deformation in asphalt layers," *Transportation Research Record: Journal of the Transportation Research Board*, vol. 537, pp. 18–30, 1975.

[34] E. N. Thrower, "Stress invariants and mechanical testing of pavement materials," Report 810, Transport and Road Research Laboratory, Crowthorne, UK, 1978.

[35] C. L. Monismith, R. G. Hicks, F. N. Finn et al., *SHRP-A-415: Permanent Deformation Response of Asphalt Aggregate Mixes*, National Research Council, Washington, DC, USA, 1994.

[36] A. Shenoy and P. Romero, "Superpave shear tester as a simple standardized measure to evaluate aggregate-asphalt mixture performance," *Journal of Testing and Evaluation*, vol. 29, no. 5, pp. 472–484, 2001.

[37] P. Romero and R. M. Anderson, "Variability of asphalt mixture tests using Superpave shear tester repeated shear at constant height test," *Transportation Research Record: Journal of the Transportation Research Board*, vol. 1767, no. 1, pp. 95–101, 2001.

[38] J. Zhang, H. Xie, P. S. Kandhal, and R. D. Powell, "Field validation of superpave shear test on ncat test track," *Journal of ASTM International*, vol. 2, no. 3, pp. 1–13, 2005.

[39] J. B. Sousa and C. L. Monismith, "Dynamic response of paving materials," *Transportation Research Record: Journal of the Transportation Research Board*, vol. 1136, pp. 57–68, 1987.

[40] E. J. Rueda, S. Caro, B. Caicedo, and J. Monroy, "A new approach for the advanced mechanical characterisation of asphalt mixtures using the hollow cylinder methodology," *Measurement*, vol. 103, pp. 333–342, 2017.

[41] K. Sokolov, R. Gubler, and M. N. Partl, "Extended numerical modeling and application of the coaxial shear test for asphalt pavements," *Materials and Structures*, vol. 38, no. 279, pp. 515–522, 2005.

[42] J. Zak, C. L. Monismith, E. Coleri, T. John, and Harvey, "Uniaxial shear tester—test method to determine shear properties of asphalt mixtures," *Journal of the Association of Asphalt Paving Technologists*, vol. 85, pp. 109–130, 2016.

[43] Y. Bi and L. Sun, "Research on test method of asphalt mixture's shearing properties," *Journal of Tongji University*, vol. 33, no. 8, pp. 1036–1040, 2005, in Chinese.

[44] T. Huang, "The research on testing method for shear performance of asphalt mixture," Master's dissertation, Changsha University of Science and Technology, Changsha, China, 2009.

[45] B. A. I. Yun-feng, "Research on application of pure torsional shear test on the shear performance evaluation of asphalt mixture," Doctoral dissertation, Dalian University of Technology, Dalian, China, 2015.

[46] J. Xie and J.-W. Wang, "Study on torsional shear test method for asphalt mixture under normal stress condition," *Journal of Highway and Transportation Research and Development*, vol. 34, no. 7, pp. 80–86, 2017, in Chinese.